Wijekoon *et al.*
CABI Agriculture and Bioscience (2024) 5:40
https://doi.org/10.1186/s43170-024-00241-2

CABI Agriculture and Bioscience

RESEARCH

Open Access

Seasonal forecasting of *Bactrocera dorsalis* Hendel, 1912 (Diptera: Tephritidae) in bioclimatic zones of Sri Lanka using the SARIMA model

W. M. C. D. Wijekoon[1*], G. A. S. M. Ganehiarachchi[2], H. C. E. Wegiriya[1] and S. P. Vidanage[2]

Abstract

Bactrocera dorsalis Hendel is a severe fruit pest that causes significant economic losses globally. Despite *B. dorsalis* having been distributed mostly across Asia, studies on its current and future density variation in Sri Lanka are sparse to date. The present study was thus carried out to assess the contemporary density variation (2020–2022) and future density fluctuation (2023–2025) of *B. dorsalis* in bioclimatic zones of Sri Lanka. The density was assessed using the monthly-based fruit fly trap collection method from randomly selected 40 locations in all bioclimatic zones (wet, intermediate, dry, and arid). The SARIMA modelling technique was applied for delineating the best-fit model and for density forecasting in each bioclimatic zone. The density variations were depicted for the year and for the bioclimatic zone (2020–2025) by colour intensity maps using QGIS. According to the findings, *B. dorsalis* shows a seasonal component to its year-round density variation and an ascending trend in its density from 2020 to 2025. Density forecasting records a 20%, 30%, 26%, and 37% density increase in the wet, intermediate, dry, and arid zones, respectively, in 2025. In 2025, the highest predicted *B. dorsalis* density from the arid zone and the lowest predicted density from the wet zone were recorded. This study contains the first forecasting attempt for *B. dorsalis* density using the SARIMA approach as well as the application of colour-intensity depiction for its density variation in Sri Lanka, which leads decision makers and stakeholders in economic agriculture to plan the scientific management of *B. dorsalis* to avoid its current and potential future threat to the country's fruit industry.

Keywords Fruit flies, Density, Future prediction, Asia

*Correspondence:
W. M. C. D. Wijekoon
chandanadammika1984@gmail.com
Full list of author information is available at the end of the article

Introduction

Fruit flies (Diptera: Tephritidae) are a group of important insect pest. Most fruit flies are polyphagous, and they cause severe economic loss by damaging many horticulture products, especially fruits and vegetables, in the tropical region (White and Elson 1994; Clarke et al. 2005; Wei et al. 2019; Peng et al. 2020). Among them, *B. dorsalis* is considered a severe fruit pest worldwide (Wei et al. 2019; Peng et al. 2020), as well as being classified as a level 1 quarantine pest by many countries (Liu et al. 2019; CABI 2021). This species has a very high invasive capability, and hence its damage has been reported up to 100% for many economically important fruit types, resulting in huge economic loss (Ekesie et al. 2009; Liendo et al. 2018; CABI 2021). A widespread distribution of *B. dorsalis* is reported throughout Asia, with limited distribution in Pacific and African regions (Aketarawong et al. 2007; Drew and Romig 2013; Choudhary et al. 2016).

The presence of *B. dorsalis* in Sri Lanka has been reported by studies in Sri Lanka (Dhanapala 1996; Anonymous 2012; Karunarathna and Karunarathna 2015; Heshani and Sirisena 2017; Ranaweera et al. 2017; Marasinghe et al. 2018; Wijekoon et al. 2021, 2022, 2023) and several other outside reports (Tsuruta et al. 2005; Drew and Romig 2013; Leblanc et al. 2018; Plant Health Australia 2018).

Sri Lanka is a tropical country, and its climatic conditions are favourable for high floral and faunal diversity. Based on the climatic factors, Sri Lanka is divided into four main bioclimatic zones: wet, intermediate, dry, and arid. The distribution of *B. dorsalis* as the predominant fruit fly species in all bioclimatic zones of Sri Lanka was reported by Wijekoon et al. (2023).

In several countries outside of Sri Lanka, forecasting models have been extensively used for the prediction of tephritid populations (Worner 1988; Yonow and Sutherst 1998; Sutherst et al. 2000; Vera et al. 2002; Stephens et al. 2007), and especially for *B. dorsalis* density by Dong et al. (2022). SARIMA (Seasonal Autoregressive Moving Average) is a seasonal time series forecasting model that is commonly used for studying spatial variability through time (Andrew 1994). This model has been extensively applied to forecast population growth with a seasonal component. The Box-Jenkins methodology is referred to as the systematic method to identify, fit, and check the data set in the SARIMA time series models (Cooray 2008). This model is scientifically vital to predict insect pest density, which is of agro-ecological significance. Though the application of SARIMA forecasting of time series has been reported in several studies in other countries (Saboia 1997; He and Lv 1992; Fan and Lv 1997; Meng 1997; Yang 2008; Zeng and Quanpeng 2011; Sanchez et al. 2013; Adebiyi et al. 2014; Unnikrishnan and Suresh 2016; Wang et al. 2016; Guo et al. 2020; Sun et al. 2020; Duan 2021; Hu & Wu 2021; Lin-feng 2021), few records have been reported in Asia (Narava et al. 2022).

To date, no study has been carried out to determine the density variation and forecasting of *B. dorsalis* in Sri Lanka. As the first attempt in Sri Lanka, the use of the SARIMA model to forecast *B. dorsalis* population is vital for agriculture stakeholders to determine the advent and patterns of *B. dorsalis* density over time and the timely intervention of proper pest control methods before damage occurs. Moreover, the outputs of the SARIMA application will be helpful to comprehend the contest of *B. dorsalis* behaviour and its potential future outbreak patterns in spatial scenarios. The present study was thus intended to assess the seasonal variation, modelling, and future forecasting of *B. dorsalis* density in bioclimatic zones of Sri Lanka.

Materials and methods

Study area

Sri Lanka is an island with an area of 65,610 km^2 and is located in the tropical region. This study was conducted in all four bioclimatic zones (wet, intermediate, dry, and arid) of Sri Lanka and these four major bioclimatic zones have been divided based on rainfall, temperature, and relative humidity.

Site selection and sample collection

Ten sampling locations in each bioclimatic zone and 40 locations from all four bioclimatic zones were randomly selected. The GIS (Geographical Information System) coordination data for each study location was recorded. The selected study locations are depicted in Fig. 1, and their GIS coordination is addressed in Table 1. In each location, 100 m^2 of area were selected, and a ME (methyl-eugenol) (5 cm diameter, 10 cm height, two circular openings with a 1 mm radius, and a ME-coated sponge) field trap was hung in a tree (1.5–4 m above ground level) at the centre of the selected area. Trapped flies were collected once a month from June 2020 to December 2022, replacing new ME-coated sponges in each sampling round. Collected fruit flies were put in transparent polythene bags and then brought to the laboratory in the Department of Zoology, University of Ruhuna, for identification. These specimens were identified using taxonomic keys (Prabhakar et al. 2012; Schutze 2012; Choudhary et al. 2014; Plant Health Australia 2018; Daud et al. 2020; Leblanc et al. 2021).

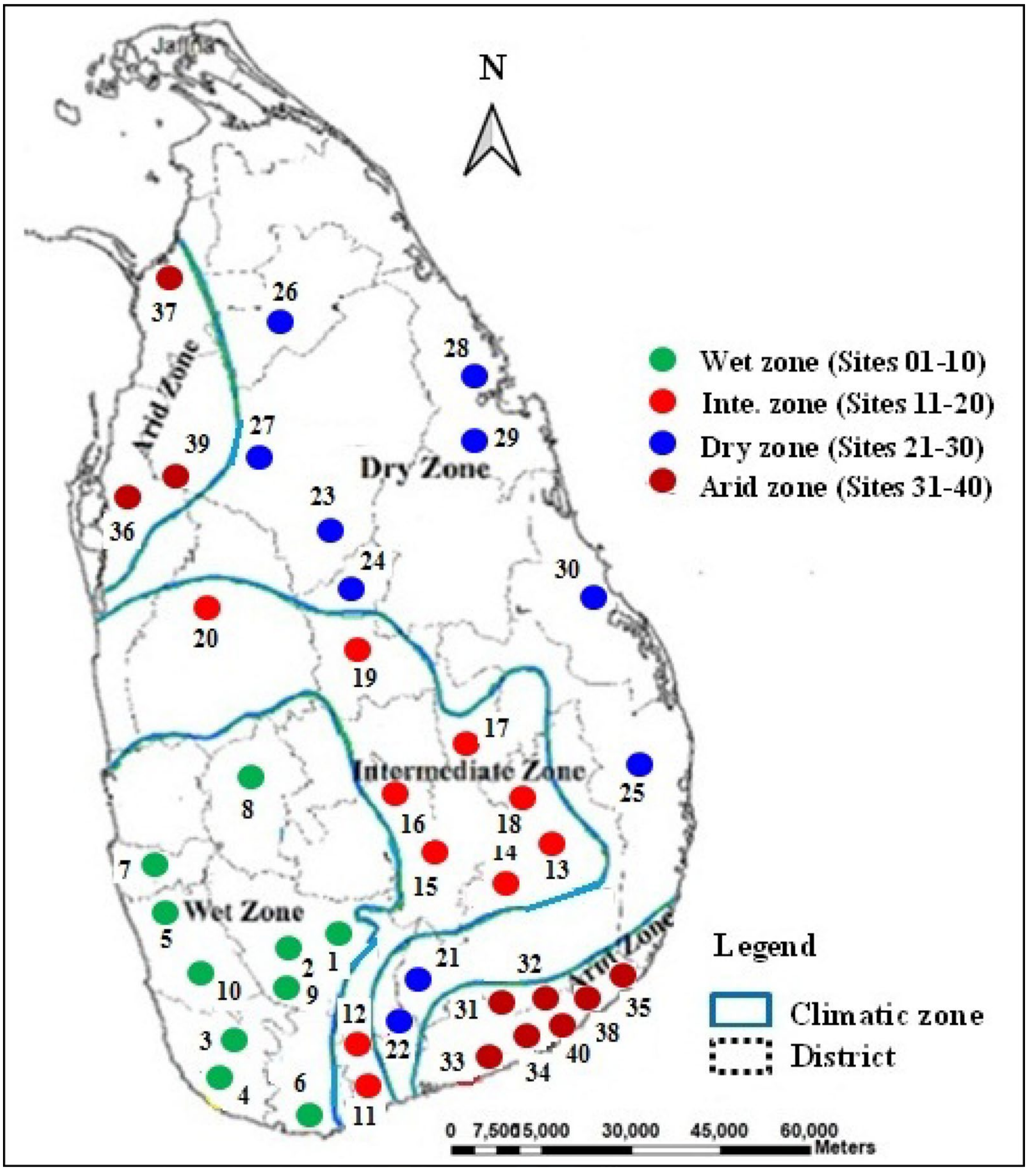

Fig. 1 Selected forty study sites in four bioclimatic zones of Sri Lanka (modified the basic map derived from Alahacoon and Edirisinghe 2021)

Data analysis

(i) Density of *B. dorsalis*

The density of recorded *B. dorsalis* was calculated using the following formula:

$$\mathbf{D} = \frac{\mathbf{l}}{\mathbf{L}}\mathbf{100},$$

where, D = density, l = number of specimens of *B. dorsalis*, L = number of all fruit fly specimens.
(ii) Spatiotemporal maps

The mean density of *B. dorsalis* in each bioclimatic zone for each study year was calculated. Then the density variations of *B. dorsalis* among bioclimatic zones for the years 2020, 2021, 2022, 2023, and 2024 were depicted by GIS maps using QGIS software (version 3.28.7, Firenze). Further, the trend of the density of *B. dorsalis* in each bio-climatic zone during the period from 2020 to 2024 was illustrated using colour intensity maps. The intensity of *B. dorsalis* density in the particular study year was depicted in graphs using "low, moderate, high, and very high" categories.

Table 1 Description of sampling localities

Number	Zone	Location	Description		
Site 1	Wet	Balangoda	6°39′ 0″ N	80° 41′ 0″ E	751 m
Site 2		Kahawaththa	7°10′0′′ N	80°36′0′′ E	679 m
Site 3		Niyagama	6°14′0′′ N	80°16′0′′ E	11 m
Site 4		Hiyare	6°07′00′′ N	80°03′33′′ E	58 m
Site 5		Horana	6°42′59′′ N	80°02′60′′ E	91 m
Site 6		Matara	5°57′17′′ N	80°33′17′′ E	12 m
Site 7		Padukka	6°50′59′′ N	80°05′18′′ E	17 m
Site 8		Ruwanwella	7°04′59′′ N	80°25′36′′ E	30 m
Site 9		Kalawana	6°48′40′′ N	80°40′14′′ E	276 m
Site 10		Matugama	6°52′19′′ N	80°11′36′′ E	24 m
Site 11	Intermediate	Agunakolaya	6°27′0′′ N	81°1′0′′ E	36 m
Site 12		Middeniya	6°14′58′′ N	80°46′02′′ E	51 m
Site 13		Monaragala	6°45′0′′ N	81°14′0′′ E	162 m
Site 14		Wellawaya	6° 44′ 15′′ N	81° 6′ 11′′ E	188 m
Site 15		Welimada	6°54′96′′ N	80°55′22′′ E	1061 m
Site 16		Hanguranketha	7°18′0′′ N	80°76′0′′ E	635 m
Site 17		Mahiyanganaya	7°33′16′′ N	81°00′36′′ E	98 m
Site 18		Bibila	6°43′0′′ N	80°46′0′′ E	262 m
Site 19		Raththota	7°51′72′′ N	80°67′15′′ E	396 m
Site 20		Nikaweratiya	7°50′48′′ N	80°20′0′′ E	210 m
Site 21	Dry	Udawalawe	6° 27′ 59′′ N	80° 52′ 59′′ E	109 m
Site 22		Barawakumbuka	6°10′0′′ N	80°49′0′′ E	44 m
Site 23		Kakirawa	8°2′31.57′′ N	80°35′37.8′′ E	142 m
Site 24		Dambulla	7° 53′ 68′′ N	80° 40′ 48′′ E	164 m
Site 25		Ampara	7°13′54′′ N	81°38′50′′ E	43 m
Site 26		Vavniya	8°73′81′′ N	80°47′71′′ E	104 m
Site 27		Anuradhapura	8°18′40′′ N	80°24′13′′ E	91 m
Site 28		Trincomalee	8°35′14′′ N	81°12′54′′ E	11 m
Site 29		Kanthale	8°22′06′′ N	81°01′41′′ E	15 m
Site 30		Batticalo	7°43′51′′ N	81°40′29′′ E	17 m
Site 31	Arid	Kithulkote	6°30′0′′ N	81°7′60′′ E	88 m
Site 32		Kudaoya	6°45′0′′ N	81°12′0′′ E	84 m
Site 33		Ambalanthota	6°7′0′′ N	81°1′0′′ E	5 m
Site 34		Debarawewa	6°17′0′′ N	81°16′0′′ E	28 m
Site 35		Kataragama	6°41′42′′ N	81°33′44′′ E	424 m
Site 36		Puththalam	8°02′26′′ N	79°50′21′′ E	5 m
Site 37		Mannar	8°98′09′′ N	79°90′44′′ E	8 m
Site 38		Tissamaharama	6°27′74′′ N	81°28′63′′ E	86 m
Site 39		Anamaduwa	7°87′77′′ N	80°01′11′′ E	64 m
Site 40		Kirinda	6°05′15′′ N	80°62′57′′ E	30 m

(iii) Seasonal ARIMA model

The following four stages were followed: *Data preparation*; plotting the density to recognize the seasonality and data proper transformations. *Model selection*; computing autocorrelation function (ACF) and partial autocorrelation function (PACF), and examining and plotting. *Estimation and diagnostics*; estimating the pattern of autocorrelations and partial autocorrelations of moving average (MA) or autoregressive (AR) based on the ACF and PACF values, based on the significance level of autocorrelations or partial autocorrelations of AR or MA, the model was considered appropriate. *Forecasting*; using the selected best-fit model.

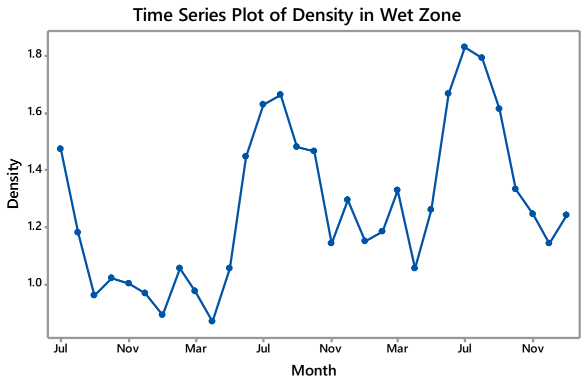

Fig. 2 Density variation of *B. dorsalis* in the wet zone (July 2020 to December 2022)

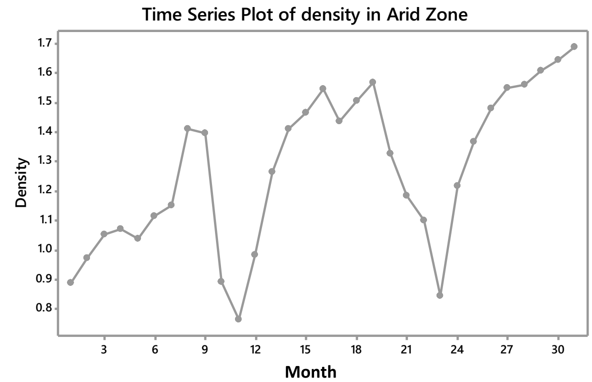

Fig. 5 Density variation of *B. dorsalis* in the arid zone (July 2020 to December 2022)

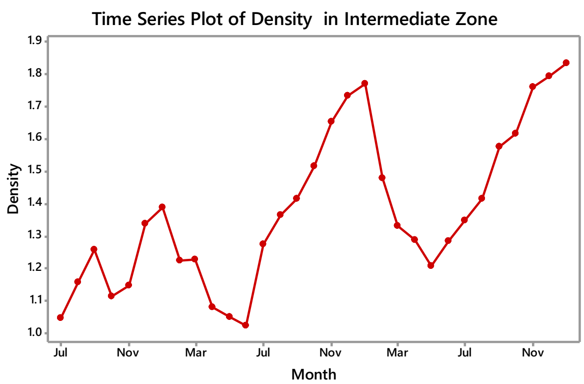

Fig. 3 Density variation of *B. dorsalis* in the intermediate zone (July 2020 to December 2022)

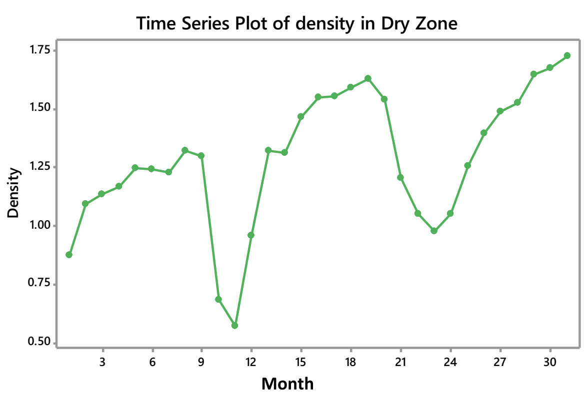

Fig. 4 Density variation of *B. dorsalis* in the dry zone (July 2020 to December 2022)

Data analysis was conducted using R (version 4.0) software. Seasonality plots, ACF and PACF plots, and residual error plots for the density of *B. dorsalis* in each bio-climatic zone were illustrated using this software.

(iv) Checking the seasonality of *B. dorsalis* density

Wet zone: Fig. 2 depicts a time series fluctuation plot of *B. dorsalis* monthly density in the wet zone from July 2020 to December 2022. The time series contains both seasonal and trend components. As a result, log-transformed data was created and used for further analysis.

Intermediate zone: Fig. 3 shows that the variance of the time series does not vary significantly, but an indistinct trend appears to begin at the end of May in 2021. Therefore, auto-correlation function (ACF) and partial auto-correlation function (PACF) plots are evaluated using log-transformed data.

Dry zone: Fig. 4 indicates that the data set has a seasonal element and a trend variation. Hence, a seasonal ARIMA model can be used to model the data. As a result, the ACF and PACF plots are first used to evaluate the model.

Arid zone: The data can be modelled using a seasonal ARIMA model since the time series plot in Fig. 5 indicates that there is a trend variation and a seasonal component.

(v) Model selection, estimation and diagnostic

Wet zone: Fig. 6 depicts the equivalent ACF and PACF. The ACF plot indicates that there is a seasonal component. There is a significant cutoff in the correlation for the PACF figure at lag 1. This means that q should be set to 1 and that the series uses the moving average (MA) (1) procedure. As a result, the seasonal ARIMA model can be used to model this series.

Intermediate zone: The plotted Fig. 7 shows the sample ACF and PACF values. Seasonality is shown in the ACF graph, and the PACF plot suggests that auto-regressive (AR) (1) might be a suitable mode

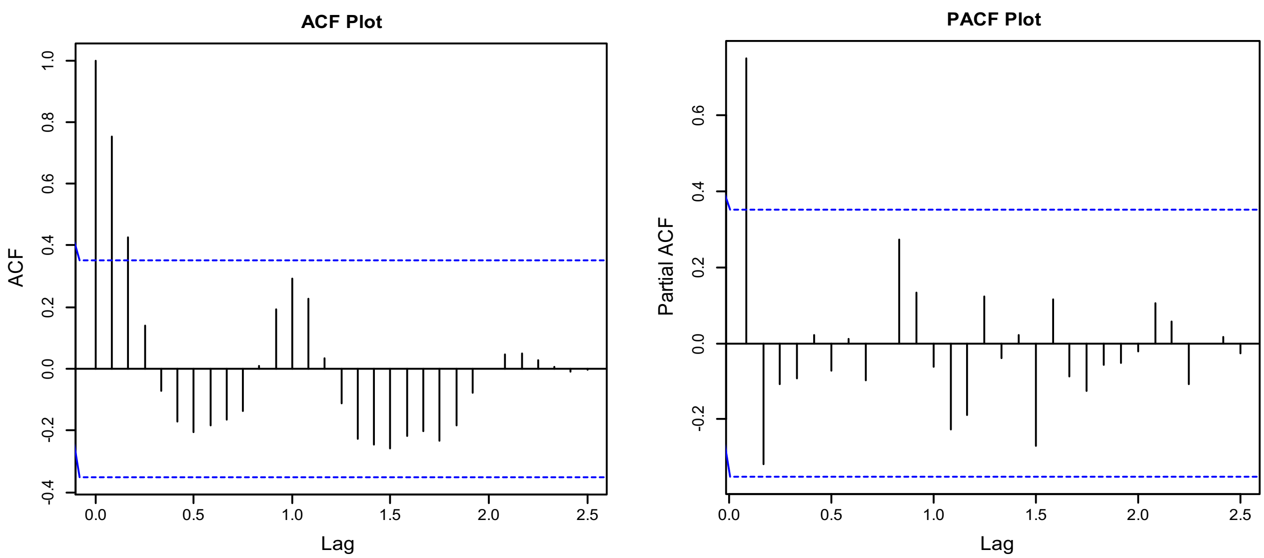

Fig. 6 Estimated sample ACF and PACF values (wet zone)

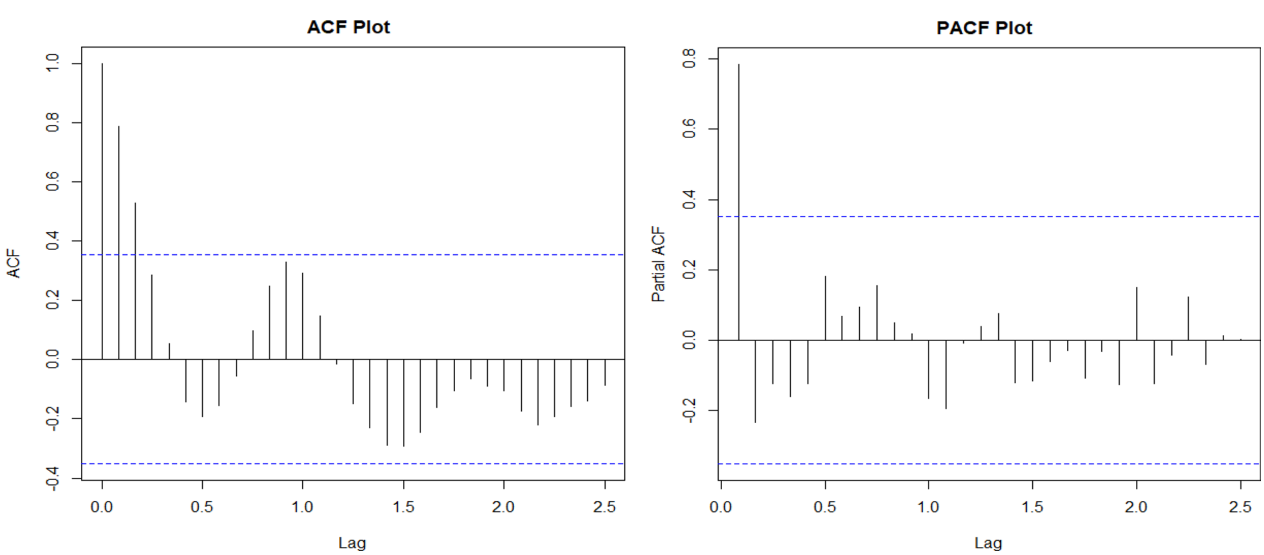

Fig. 7 Estimated sample ACF and PACF values (intermediate zone)

for the data. As a result, the seasonal ARIMA model can be used to model this series.

Dry zone: Fig. 8 shows the derived sample ACF and PACF values. The proper MA (1) model, with q = 1, is represented by the PACF graphic. As a result, the ARIMA model can be used to represent this series.

Arid zone: The seasonality component might be taken into account based on the estimated sample ACF and PACF values that are presented in Fig. 9, and the PACF plot suggests an AR (1) model.

The best-fit seasonal ARIMA model to forecast the density in each bio-climatic zone was auto-generated by the software. The ARIMA model consists of three main components, such as auto-regression (AR), moving average (MA), and integration (I) terms. This model is useful for modelling both non-seasonal (p, d, q) and a wide range of seasonal data (P, D, Q) as well as an autoregressive term denoted as AR (p), the order of differences to make the non-stationary time series stationary as (d), and the number of moving average terms as MA (q). The fitted equation for each identified best

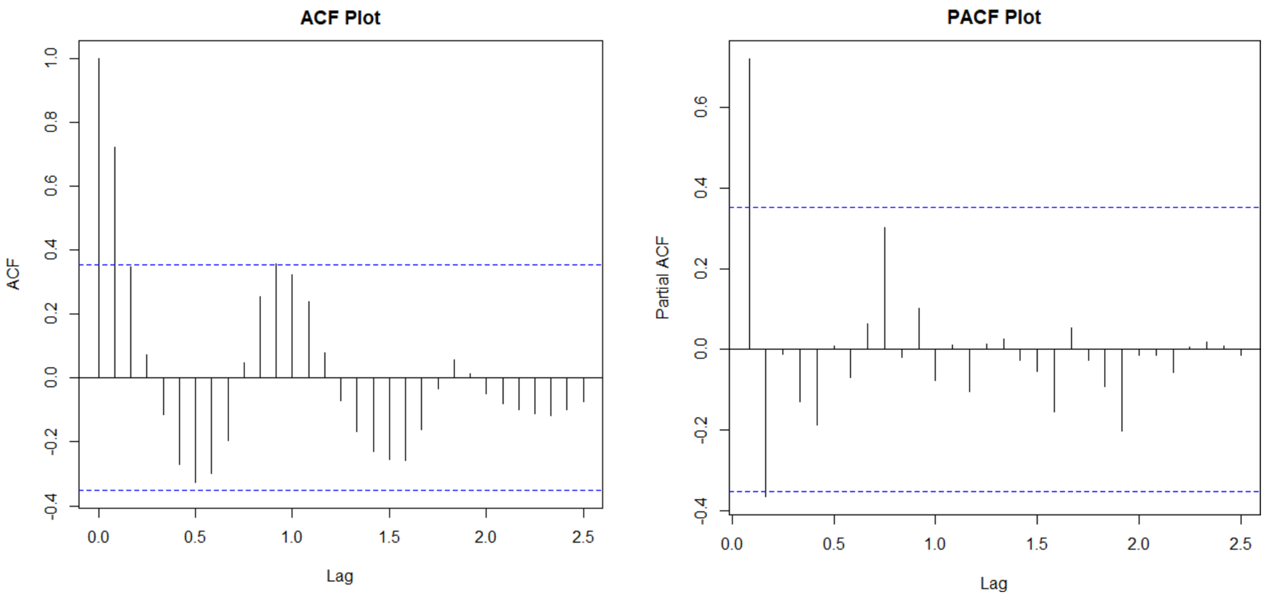

Fig. 8 Estimated sample ACF and PACF values (dry zone)

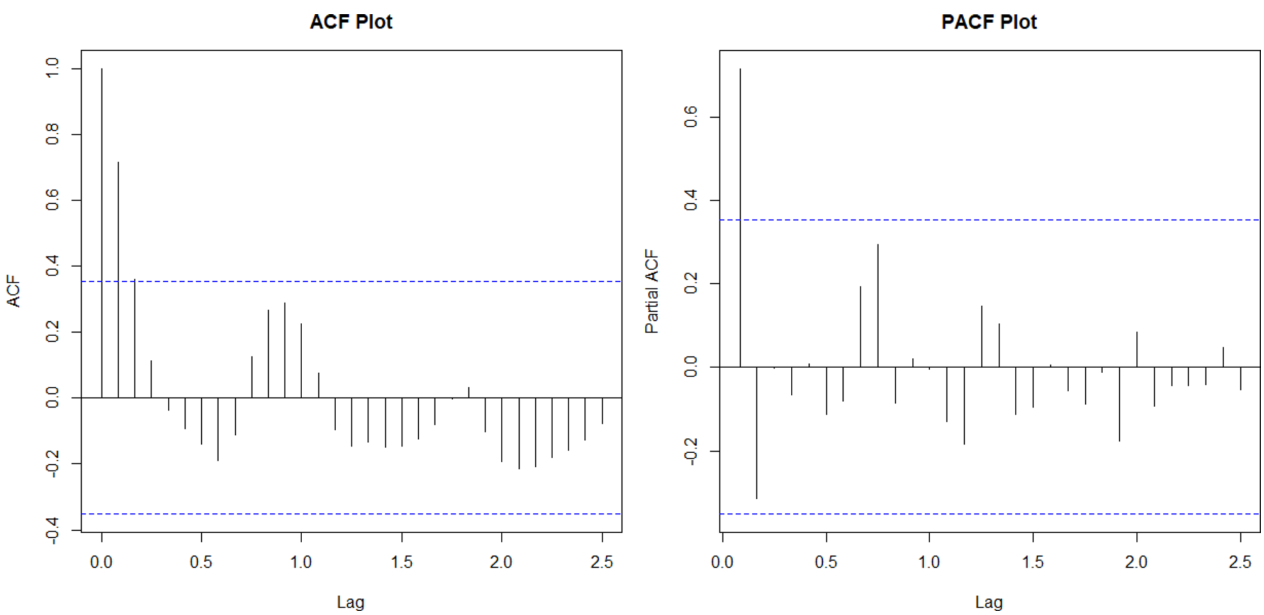

Fig. 9 Estimated sample ACF and PACF values (arid zone)

Table 2 Best fit models for forecasting the *B. dorsalis* density in bioclimatic zones

Zone	Best model	Equation	Standard error	Substituted equation
Wet	ARIMA (0, 1, 1) $(0, 1, 0)_{12}$	$(1 - B)(1 - B^{12})x_t = (1 - \beta_1 B)e_t$	– 0.1631	$(1 - B)(1 - B^{12})x_t = [1 - (-0.6132)B]e_t$
Intermediate	ARIMA (1, 1, 0) $(0, 1, 0)_{12}$	$(1 - \alpha_1 B)(1 - B)x_t = e_t$	– 0.5112	$[1 - (-0.5112)B](1 - B)x_t = e_t$
Dry	ARIMA (0, 1, 1) $(0, 1, 0)_{12}$	$(1 - B)(1 - B^{12})x_t = (1 - \beta_1 B)e_t$	– 0.6506	$(1 - B)(1 - B^{12})x_t = [1 - (-0.6506)B]e_t$
Arid	ARIMA (0, 1, 1) $(0, 1, 0)_{12}$	$(1 - B)(1 - B^{12})x_t = (1 - \beta_1 B)e_t$	– 0.6742	$(1 - B)(1 - B^{12})x_t = [1 - (-0.6742)B]e_t$

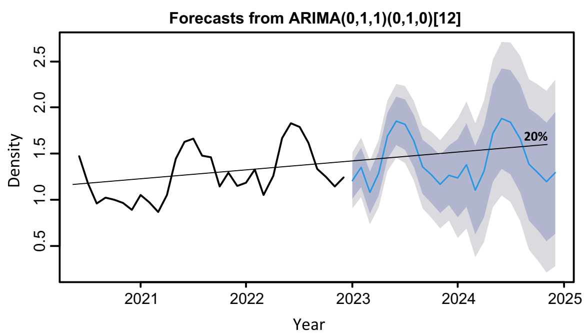

Fig. 10 Forecasting of *B. dorsalis* density for 2023 to 2025 (wet zone)

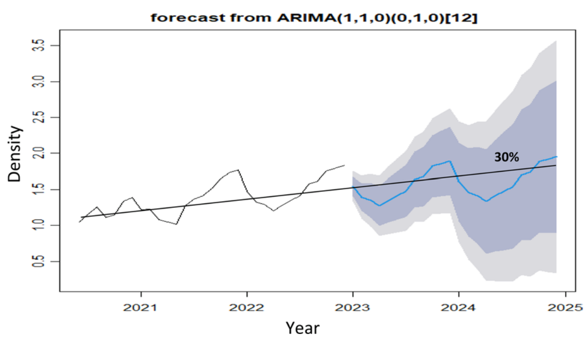

Fig. 11 Forecasting of *B. dorsalis* density for 2023 to 2025 (intermediate zone)

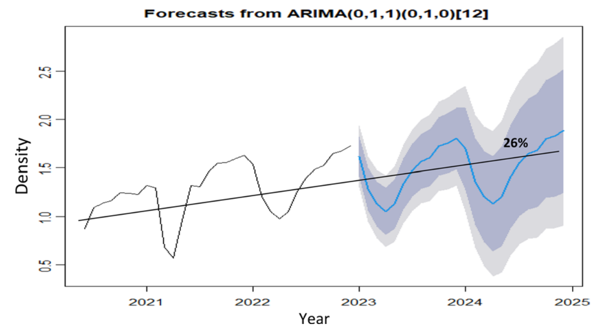

Fig. 12 Forecasting of *B. dorsalis* density for 2023 to 2025 (dry zone)

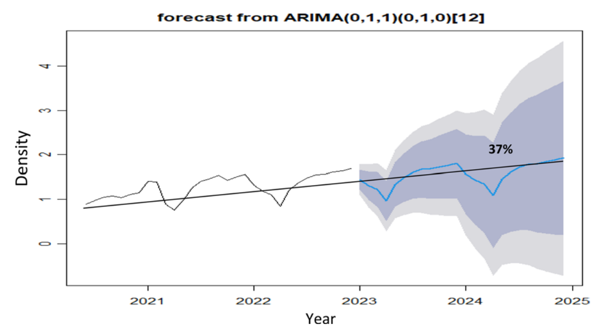

Fig. 13 Forecasting of *B. dorsalis* density for 2023 to 2025 (arid zone)

ARIMA model was created using ARIMA notations as follows:

$$\text{ARIMA} \quad \underbrace{(p,\ d,\ q)}_{\text{Non-seasonal part}} \quad \underbrace{(P,\ D, Q)s}_{\text{Seasonal part}}.$$

The representation of multiplicative seasonal ARIMA as follows,

$$\Phi_p(B^s)\phi_p(B)(1\text{-}B)^d X_t = \Theta_Q(B^s)\Theta_q(B)e_t$$

where, $\Phi_p(B^s)$ is the seasonal AR operator of order P; Φ_p is the regular AR operator of order p; $(1-B)^d X_t$ represents the seasonal differences and $d=(1-B)d$ the regular differences; $\Theta_Q(B^s)$ is the seasonal moving average operator of order Q; $\Theta_q(B)$ is the regular moving average operator of order q; e_t is a white noise process.

Results

The forecasting of the density of *B. dorsalis* are shown for each wet, intermediate, dry, and arid zone as follows:

Best fit models and residual values

According to the preceding estimations, the auto-generated best fit models for *B. dorsalis* density in the bioclimatic zones are indicated in Table 2.

Further residual plots imply that these models are fair enough in forecasting the density of *B. dorsalis* in wet, intermediate, dry and arid zones.

Forecasting of *B. dorsalis* density

Wet zone: Fig. 10 shows the *B. dorsalis* predicting density using the aforementioned model equation for the years 2023–2025. The density of *B. dorsalis* is showing an upward trend from 2020 to 2025. In comparison to 2020, a 20% increase in *B. dorsalis* density is expected in 2025.

Intermediate zone: Fig. 11 depicts a rising trend in density over time for the mean annual density of *B. dorsalis* from 2020 to 2025. In comparison to 2020, *B. dorsalis*' density could grow by 30% in 2025.

Dry zone: Fig. 12 shows an increasing trend in the mean annual density of *B. dorsalis* from 2020 to 2025. In comparison to 2020, *B. dorsalis* density increases by 26% in 2025.

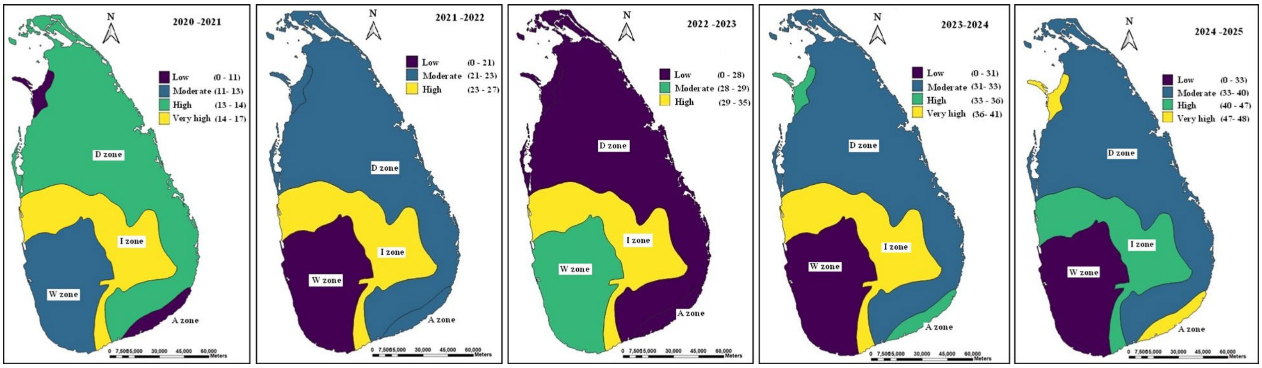

Fig. 14 The overall variation of *B. dorsalis* mean density among bioclimatic zones from 2020 to 2025

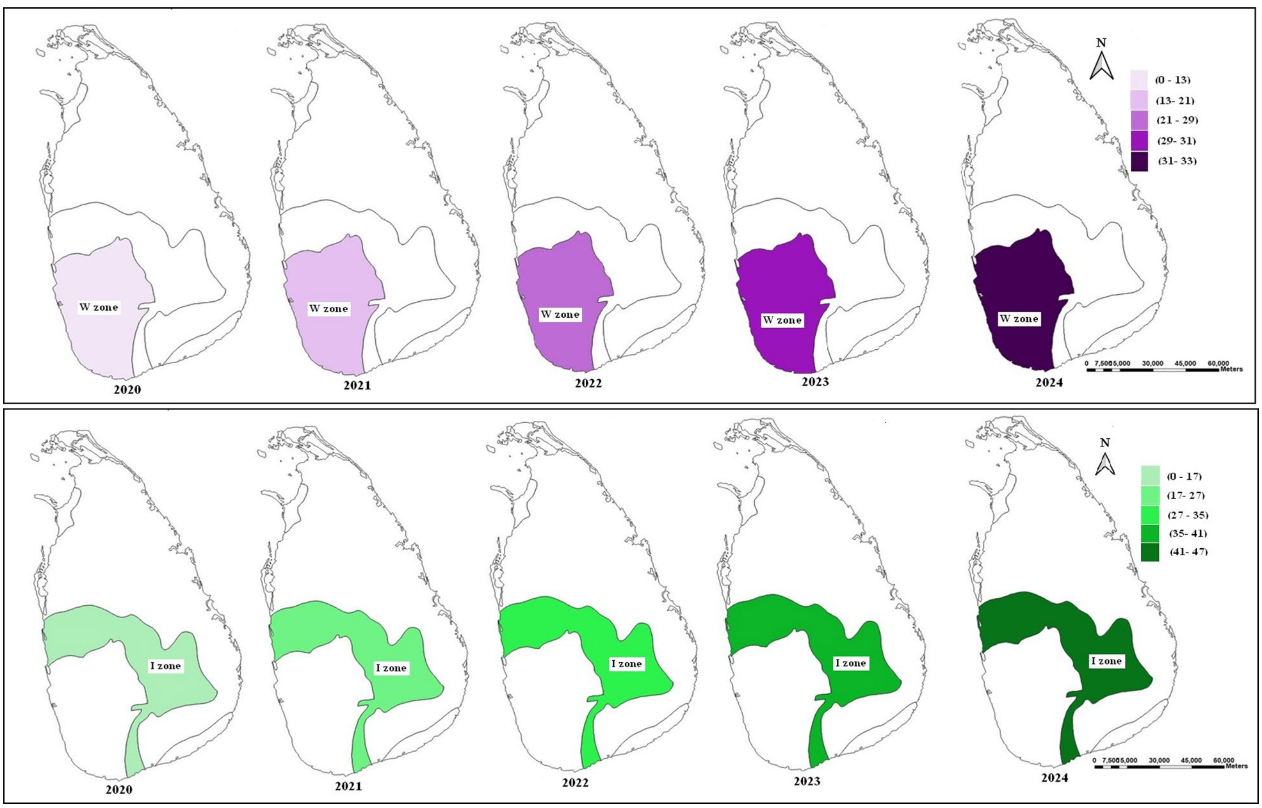

Fig. 15 Mean density variation of *B. dorsalis* from 2020 to 2025 in wet and intermediate zones (W: wet; I: intermediate)

Arid zone: Compared to the other three climate zones, the arid zone anticipates the greatest increase in *B. dorsalis* density. The density of *B. dorsalis* is on increasing, and in 2025, this upward tendency could reach 37% (Fig. 13).

Note: The colour shades on both sides of the trend curve in Figs. 10, 11, 12 and 13 indicate the level of the variation of standard deviation.

Comparison of B. dorsalis density forecasting from 2020 to 2025 for all bioclimatic zones

From 2020 to 2025, *B. dorsalis* density could increase in all bioclimatic zones. The intermediate zone from 2020 to 2024 has the maximum density of *B. dorsalis*, as seen in Fig. 14. The arid zone is expected to have the highest density between 2024 and 2025.

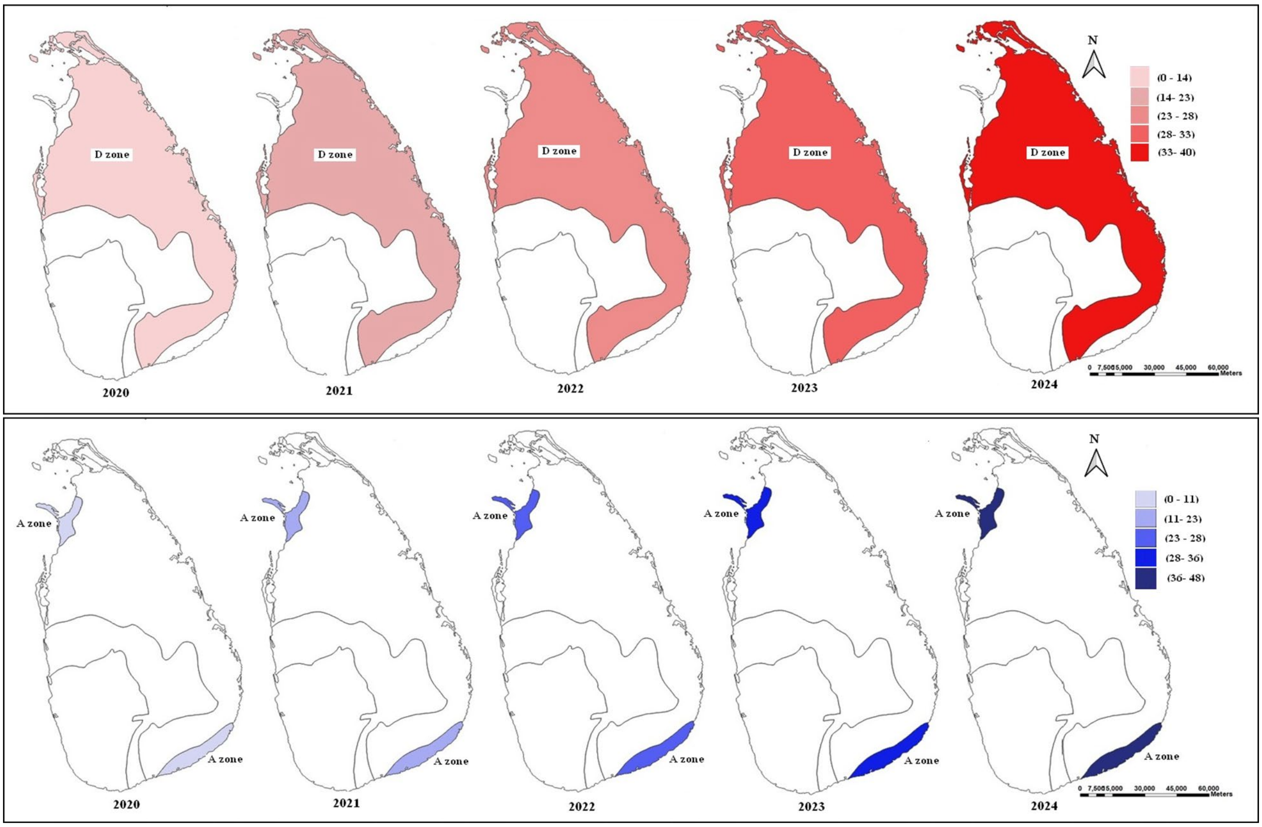

Fig. 16 Mean density variation of *B. dorsalis* from 2020 to 2025 in dry and arid zones (D: dry; A: arid)

B. dorsalis will therefore be found in the arid zone at the maximum density in 2025, despite this zone having the lowest density in 2020. *B. dorsalis* density in the wet zone was moderate in 2020, and it will be low in 2025. The ascending order of *B. dorsalis* density variation among bioclimatic zones in the specific year as: 2020–2021: Arid < Wet < Dry < Intermediate. 2021–2022: Wet < Arid < Dry < Intermediate. 2022- 2023: Arid < Dry < Wet < Intermediate. 2023-2024: Wet < Dry < Arid < Intermediate. 2024- 2025: Wet < Dry < Intermediate < Arid.

Overall density variation of B. dorsalis in each wet, intermediate, dry and arid zone during the period of 2020–2025

From 2020 to 2025, Figs. 15, 16 shows rising trends in *B. dorsalis* density variation. The intensity of the color utilized further emphasizes their ascending order.

The ascending order of *B. dorsalis* density variation in each bioclimatic zone from 2020 to 2025: Wet zone: 2020 < 2021 < 2022 < 2023 < 2024. Intermediate zone: 2020 < 2021 < 2022 < 2023 < 2024. Dry zone: 2020 < 2021 < 2022 < 2023 < 2024. Arid zone: 2020 < 2021 < 2022 < 2023 < 2024.

Discussion

The basic data analysis demonstrated that the seasonal ARIMA model is the best fit model for the data set since the density of *B. dorsalis* in all bioclimatic zones implied a seasonal component in every study year. As shown by Cooray (2008), later probability plots and residual values of each chosen model for the relevant bioclimatic zone showed the best fit for the specific data set. De Villiers et al. (2016) emphasize the need to take into account the seasonal element when calculating the density of *B. dorsalis*. They pointed out that studies frequently refer to population survival using occurrences and disregard seasonal change. De Villiers et al. (2016), contend that *B. dorsalis* exhibits a seasonal population and that identifying their advantageous seasons is essential to applying control methods to avoid significant losses to fruits, provide further support for the application of seasonal ARIMA for the current data series.

Furthermore, Dong et al. (2022) noted that because *B. dorsalis* distribution is strongly related to the seasonal conditions in the environment, investigations on its forecasts should concentrate on both its seasonal and year-round distribution.

According to Peris (2016), the main mango fruiting season corresponds with the wet period of in each bioclimatic zone. As such, the seasonality of *B. dorsalis* density in each bioclimatic zone is mostly determined by the fruiting season and the wet period. Chen et al. (1995), Lv et al. (2008), Patel et al. (2013), Bana et al. (2017) and Momen et al. (2022), all support the current finding by revealing that the seasonal variation of *B. dorsalis* closely correlates with the harvesting periods of their main host plant.

The arid zone is expected to have the highest *B. dorsalis* density in 2025, indicating a high risk to the zone's future fruit sector. The wet zone had the lowest expected density of *B. dorsalis* in 2025, which suggests that the probability of risk is decreasing for wet zone fruits in the future. It further shows the possibility of *B. dorsalis* density variations over time among Sri Lanka's bioclimatic zones between 2020 and 2025. Intriguingly, in the arid zone, *B. dorsalis* exhibited the lowest density in 2020, and by 2025, its highest density may be predicted. Despite a notable increase in *B. dorsalis* density being observed in the intermediate zone for the years 2020–2022, their predicted density from 2023–2025 stays moderate. Interestingly, the population of *B. dorsalis* in the wet zone decrease noticeably from 2020 to 2025. These findings may be explained by significant behavioral characteristics of *B. dorsalis*, including its propensity for rapid invasion, broad distribution, and potential environmental climate tolerance (Loomans et al. 2019).

This foremost, but valuable, study results make it important for agriculture authorities and farmers in Sri Lanka to take necessary precautions to control the *B. dorsalis* populations to avoid serious economic loss in the future fruit industry in Sri Lanka. This astounding findings can be further useful for designing, planning, and implementing proper scientific control measures in managing future *B. dorsalis* devastating fruit damages in the bioclimatic zones of Sri Lanka.

Conclusions

Bactrocera dorsalis shows a year-round density variation with a seasonal component. *B. dorsalis* would have an upward density trend from 2020 to 2025. The forecast density increase of *B. dorsalis* is 20%, 30%, 26%, and 37%, respectively, in the wet, intermediate, dry, and arid zones. The highest *B. dorsalis* density from the arid zone and the lowest from the wet zone could be predicted in 2025.

Acknowledgements
Dr. H. L. Jayetileke and Dr. K. D. Prasangika, Department of Mathematics, University of Ruhuna, Matara, Sri Lanka for their great supports to analyze the data set.

Author contributions
W. M. C. D. Wijekoon conducted field surveys, data collection, data entering, data analysis and writing the manuscript, G.A.S.M. Ganehiarachchi, H. C. E. Wegiriya & S. P. Vidanage supervised the research and reviewed the manuscript. The authors agree that the submitted work has not been published previously, that the work is not under consideration for publication elsewhere and that all authors agree to the publication of this work.

Funding
The study was conducted on self-funding and there was no any external funding source at the time of submitting the manuscript.

Availability of data and materials
The study included in the manuscript was based on the work carried out for a postgraduate degree. The results will be included in the thesis and to be submitted future to the Faculty of Graduate Studies, University of Kelaniya, Sri Lanka.

Declarations

Competing interests
The authors would like to declare that there are no conflicts of interest in undertaking this research.

Author details
[1]Department of Zoology, University of Ruhuna, Matara, Sri Lanka. [2]Department of Zoology and Environmental Management, University of Kelaniya, Kelaniya, Sri Lanka.

Received: 13 October 2023 Accepted: 29 March 2024
Published online: 18 April 2024

References
Adebiyi AA, Adewumi AO, Ayo CK. Comparison of ARIMA and artificial neural networks models for stock price prediction. J Appl Math. 2014;2014(2014):1–7.
Aketarawong N, Bonizzoni M, Thanaphum S, Gomulski LM, Gasperi G, Malacrida AR, Gugliemino CR. Inferences on the population structure and colonization process of the invasive oriental fruit fly, *Bactrocera dorsalis* (Hendel). Mol Ecol. 2007;16:3522–32. https://doi.org/10.1111/j.1365-294X.2007.03409.x.
Alahacoon N, Edirisinghe M. Spatial variability of rainfall trends in Sri Lanka from 1989 to 2019 as an indication of climate Change. ISPRS Int J Geo-Informat. 2021;10:1–84. https://doi.org/10.3390/ijgi10020084.
Andrew CH. Forecasting structural time series and the Kalman filter. Cambridge: Cambridge University Press; 1994. p. 1–234.
Anonymous. Amba Wagawa (mango cultivation). Department of Agriculture, Colombo (In Sinhala/Tamil), 2012.
Bana JK, Hemant S, Sushil K, Pushpendra S. Impact of weather parameters on population dynamics of oriental fruit fly, *Bactrocera dorsalis* (Hendel) (Diptera: Tephritidae) under south Gujarat mango ecosystem. J Agrometeorol. 2017;19(1):78–80. https://doi.org/10.54386/jam.v19i1.762.
CABI. *Bactrocera dorsalis* (Oriental fruit fly): Invasive Species Compendium . Available at: https://www.cabi.org/isc/datasheet/17685. 2021, Accessed 25 May 2023.
Chen HD, Zhou CQ, Yang PJ, Liang GQ. On the seasonal population dynamics of melon and oriental fruit flies and pumpkin fly in Guangzhou area. J Plant Protect. 1995;22:348–54 (**in Chinese**).
Choudhary JS, Naaz N, Prabhakar CS, Lemtur M. Genetic analysis of oriental fruit fly, *Bactrocera dorsalis* (Diptera: Tephritidae) populations based on mitochondrial cox1 and nad1 gene sequences from India and other Asian countries. Genetica. 2016;144:611–23. https://doi.org/10.1007/s10709-016-9929-7.
Choudhary JS, Naaz N, Prabhakar CS, Das B, Maurya S, Kumar S. Field guide for identification of fruit fly species of genus *Bactrocera* prevalent in and around mango orchards. Technical booklets No.: R-43/Ranchi-16. ICAR

Research Complex for Eastern Region, Research Centre, Ranchi. 2014; p.1–16.

Clarke AR, Armstrong KF, Carmichael AE, Milne JR, Raghu S, Roderick GK, Yeates DK. Invasive phytophagous pests arising through a recent tropical evolutionary radiation: the *Bactrocera dorsalis* complex of fruit flies. Annu Rev Entomol. 2005;50:293–319. https://doi.org/10.1146/annurev.ento.50.071803.130428.

Cooray TMJA. Applied time series analysis and forecasting. Narosa Publishing House Pvt Ltd., 22 Delhi Medical association Road, Daryaganj, New Delhi, 2008, 110002. p. 1–294.

Daud ID, Melina Dayanara HK, Mustika T. Fruit fly identification from fruits and vegetables of Turikale Maros, South Sulawesi, Indonesia. In: Advances in biological sciences research. International Conference and the 10th Congress of the Entomological Society of Indonesia (ICCESI 2019), 2020;8: 94–100.

De Villiers M, Hattingh V, Kriticos DJ, Brunel S, Vayssières JF, Sinzogan A, Billah MK, Mohamed SA, Mwatawala M, Abdelgader H. The potential distribution of *Bactrocera dorsalis*: considering phenology and irrigation patterns. Bull Entomol Res. 2016;106:19–33.

Dhanapala MG. Control of fruit flies using methyl eugenol traps. In: Second International Congress of Entomological Sciences at PARC. Islamabad, Pakistan. 1996, p. 64–65.

Dong Z, He Y, Ren Y, Wang G, Chu D. Seasonal and year-round distributions of *Bactrocera dorsalis* (Hendel) and its risk to temperate fruits under climate change. Insects. 2022;13:500–50. https://doi.org/10.3390/insects13060550.

Drew RAI, Romig MC. Tropical fruit flies of South-East Asia. Wallingford: CABI; 2013. p. 655p.

Duan G. Research on bit coin price forecast based on ARIMA model. Modern Marketing. 2021;491:27–9.

Ekesi S, Billah MK, Nderitu PW, Lux SA, Rwomushana I. Evidence for competitive displacement of *Ceratitis cosyra* by the invasive fruit fly *Bactrocera invadens* (Diptera: Tephritidae) on mango and mechanisms contributing to the displacement. J Econ Entomol. 2009;102:981–91. https://doi.org/10.1603/029.102.0317.

Fan J, Lv Y. Bayes modeling and prediction of AR (p) sequence with ellipsoid distribution. J Eng Math. 1997;4(1):65–70.

Guo S, Yan P, Haokun E. Short-term prediction of power consumption in Beijing based on ARIMA model. J Beijing Informat Sci Technol Univ (Nat Sci Edn). 2020;35(5):93–6.

He B, Lv T. +e seasonal ARIMA model of monthly runoff series. J Zhongyuan Inst Technol. 1992;4(3):47–53.

Heshani DKA, Sirisena UGAI. Diversity of fruit flies (Diptera: Tephritidae) in selected locations in the dry zone of Sri Lanka. In: Symposium on crop protection and improvement. 2017, p. 68.

Hu Y, Wu J. Analysis and prediction of spatial characteristics of precipitation based on ARIMA model. Jiangxi Sci. 2021;39(10):99–104.

Karunaratne MMSC, Karunaratne UKPR. Factors influencing the responsiveness of male oriental fruit fly, *Bactrocera dorsalis*, to methyl eugenol (3,4 di-methoxyalyl benzene). Trop Agric Res Ext. 2015;15(4):92–7. https://doi.org/10.4038/tare.v15i4.5258.

Leblanc L, Doorenweerd C, Jose MS, Sirisena UGAI, Hemachandra KS, Rubinoff D. Description of a new species of *Dacus* from Sri Lanka, and new country distribution records (Diptera, Tephritidae, Dacinae). ZooKeys. 2018;795:105–14. https://doi.org/10.3897/zookeys.795.29140.

Leblanc L, Hossain MA, Momen M, Seheli K. New country records, annotated checklist and key to the *Dacine* fruit flies (Diptera: Tephritidae: Dacinae: Dacini) of Bangladesh. Insecta Mundi. 2021;880:1–56.

Liendo MC, Mariac L, Maria A, Parreno J, Cladera M, Ariat V, Diego FS. Coexistence between two fruit fly species is supported by the different strength of intra- and interspecific competition. Ecolog Entomol. 2018;43(3):294–303. https://doi.org/10.1111/een.12501.

Lin-feng S. Research on vanke's stock closing price based on ARIMA model. Trade Fair Econ. 2021;4(3):50–2.

Liu H, Dong-ju Z, Yi-juan XU, Lei W, Dai-feng C, Yi-xiang QI, Ling Z, Yongyue LU. Invasion, expansion, and control of *Bactrocera dorsalis* (Hendel) in China. J Integr Agric. 2019;18(4):771–87. https://doi.org/10.1016/S2095-3119(18)62015-5.

Loomans A, Makrina D, Mart K, Martijn S, Sybren V. Pest survey card on *Bactrocera dorsalis*. EFSA Support Publ. 2019;16(9):2–25. https://doi.org/10.2903/sp.efsa.2019.en-1714.

Lv X, Han SC, Xu JL, Hang H, Wu H, Ou JF, Sun L. Population dynamics of *Bactrocera dorsalis* (Hendel) in Guangzhou, Guangdong Province, with analysis of the climate factors. Acta Ecol Sin. 2008;28:1850–6 (**in Chinese**).

Marasinghe JP, Madugalle S, Nugapitiya CAK, Harischandra YRN, Hettiarachchi AK. The seasonal abundance of fruit fly species in Sri Lanka and the male annihilation technique as a control measure for fruit flies; two case studies. Trop Agric. 2018;166(4):33–50.

Meng Z. New information prediction of multidimensional ARMA (p, q) sequences. J Eng Math. 1997;4(3):125–8.

Momen M, Hossain F, Hossain MAA, Seheli K. Population fluctuation of economically important male dacine fruit flies (Diptera: Tephridae) at savaar, Dhaka. J Entomol Zool Stud. 2022;10(3):19–27. https://doi.org/10.2227/j.ento.2022.v10.i3a.9007.

Narava R, Sai Ram K, Jagdish DV, Anil KP, Ranga RGV, Srinivasa RV, Suraj PM, Vinod K. Development of temporal model for forecasting of *Helicoverpa armigera* (Noctuidae: Lepidopetra) Using ARIMA and Artificial Neural Networks. J Insect Sci. 2022;22(3):2. https://doi.org/10.1093/jisesa/ieac019.

Patel KB, Saxena SP, Patel KM. Fluctuation of fruit fly oriented damage in mango in relation to major abiotic factors. Hort Flora Res Spectrum. 2013;2(3):197–201.

Peng W, Yu S, Handler AM, Tu Z. miRNA-1-3p is an early embryonic male sex-determining factor in the Oriental fruit fly *Bactrocera dorsalis*. Nat Commun. 2020;11(1):23–35. https://doi.org/10.1038/s41467-020-14622-4.

Peris K. The mango in the democratic socialist republic of Sri Lanka. Mango Tree Encyclopaedia. 2016;19:337–70.

Plant Health Australia. The Australian handbook for the identification of fruit flies. Version 3.1. Plant Health Australia. Canberra, ACT. 2018, p. 1–162.

Prabhakar CS, Sood P, Mehta PK. Pictorial keys for predominant *Bactrocera* and *Dacus* fruit flies (Diptera: Tephritidae) of north western Himalaya. Arthropods. 2012;1(3):101–11.

Ranaweera PH, Ranathunga M, Nugaliyadde L, Hemachandra KS, Rajapakshe M, Erabadupitiya HRUT, Wijesekara LK, Edirisinghe EMRD. Abundance and Species Richness of fruit flies (Diptera: Tephritidae) in Major cucurbit growing areas in Anuradhapura, Kurunegala and Kandy District in Sri Lanka and farmers' perception on recommended management methods. Annals of Sri Lanka Department of Agriculture. 2017;19: 98–112.

Saboia JLM. Autoregressive integrated moving average (ARIMA) models for birth forecasting. J Am Stat Assoc. 1977;72(358):264–70.

Sanchez AB, Ordoñez C, Lasheras FS. Forecasting SO_2 pollution incidents by means of elman artificial neural networks and ARIMA models. Abstr Appl Anal. 2013;2013:1–6.

Schutze MK. Population structure of *Bactrocera dorsalis* ss, *B. papayae* and *B. philippinensis* (Diptera: Tephritidae) in Southeast Asia: evidence for a single species hypothesis using mitochondrial DNA and wing-shape data. BMC Eval Biol. 2012;12:1.

Stephens AEA, Kriticos DJ, Leriche A. The current and future potential geographic distribution of the Oriental fruit fly, *Bactrocera dorsalis*, (Diptera: Tephritidae). Bull Entomol Res. 2007;97:369–78. https://doi.org/10.1017/S0007485307005044.

Sun X, Gao Y, Yuan X. Analysis and prediction of birth rate in China. J Shanxi Normal Univ (Philos Soc Sci Edn). 2020;35(3):256–64.

Sutherst RW, Collyer BS, Yonow T. The vulnerability of Australian horticulture to the Queensland fruit fly, *Bactrocera* (Dacus) *tryoni*, under climate change. Aust J Agric Res. 2000;51:467–80.

Tsuruta K, Bandara HMJ, Rajapakse GBJP. Notes on the lure responsiveness of fruit flies of the tribe dacini (Diptera: Tephritidae) in Sri Lanka. Esakia. 2005;45:179–84. https://doi.org/10.5109/2707.

Unnikrishnan J, Suresh KK. Modelling the impact of government policies on import on domestic price of Indian gold using ARIMA intervention method. Int J Math Math Sci. 2016; 1–6.

Vera MT, Rodriguez R, Segura DF, Cladera JL, Sutherst RW. Potential geographical distribution of the Mediterranean fruit fly, *Ceratitis capitata* (Diptera: Tephritidae), with emphasis on Argentina and Australia. Environ Entomol. 2002;31:1009–22.

Wang H, Liu L, Dong S. A novel work zone short-term vehicle-type specific traffic speed prediction model through the hybrid EMD-ARIMA framework. Transport Bus Transport Dynam. 2016;4(3):159–86.

Wei DD, He W, Lang N, Miao ZQ, Xiao LF, Dou W, Wang JJ. Recent research status of *Bactrocera dorsalis*: insights from resistance mechanisms and population structure. Arch Insect Biochem Physiol. 2019;102(3):2015–9. https://doi.org/10.1002/arch.21601.

White IM, Elson-Harris M. Fruit flies of economic significance their identification and bionomics. Wallingford, UK: CAB International, 1994. p. 433.
Wijekoon WMCD, Ganehiarachchi GASM, Wegiriya HCE, Vidanage SP. The variation of abundance and fruit damage of *Bactrocera dorsalis* on two commercial varieties of *Mangifera indica* in main Bio-climatic Zones of Sri Lanka. Sri Lankan J Agric Ecosyst. 2022;4(1):149–64. https://doi.org/10.4038/sljae.v4i1.75.
Wijekoon WMCD, Ganehiarachchi GASM, Wegiriya HCE, Vidanage SP. The status of *Bactrocera dorsalis* as an emerging predominant pest in the commercial fruit industry in Sri Lanka. Trop Agric Res Ext. 2023;26(1):80–7.
Wijekoon WMCD,Ganehiarachchi GASM, Wegiriya HCE, Vidanage SP. Infestation and emergence of *Bactrocera dorsalis* (Diptera: Tephritidae) on two varieties of *Mangifera indica* from selected locations in wet zone and dry zone of Sri Lanka, International conference of Applied and Pure Sciences, University of Kelaniya, 2021, p. 18.
Worner SP. Eco-climatic assessment of potential establishment of exotic pests. J Econ Entomol. 1988;81:973–83.
Yang J. Modeling and forecasting of electricity consumption time series based on ARIMA model. J Eng Math. 2008;4(4):611–5.
Yonow T, Sutherst RW. The geographical distribution of the Queensland fruit fly, *Bactrocera* (Dacus) *tryoni*, in relation to climate. Aust J Agric Res. 1998;49:935–53.
Zeng Q, Quanpeng JZ. Short-term traffic flow prediction based on BP neural network and ARIMA. J Zhengzhou Univ. 2011;32(4):60–3.

Publisher's Note